Stress concentrations in nanoscale defective graphene

Congwei Wang, Junzhong Wang, and Asa H. Barber

Citation: AIP Advances **7**, 115001 (2017); doi: 10.1063/1.4996387
View online: https://doi.org/10.1063/1.4996387
View Table of Contents: http://aip.scitation.org/toc/adv/7/11
Published by the American Institute of Physics

Stress concentrations in nanoscale defective graphene

Congwei Wang,[1,2] Junzhong Wang,[1] and Asa H. Barber[2,3,a]
[1]*CAS Key Laboratory of Carbon Materials, Institute of Coal Chemistry, Chinese Academy of Sciences, Taiyuan 030001, P. R. China*
[2]*School of Engineering and Materials Science, Queen Mary University of London, Mile End Road, London E1 4NS, U.K.*
[3]*School of Engineering, University of Portsmouth, Portsmouth PO1 3DJ, U.K.*

(Received 5 May 2017; accepted 10 October 2017; published online 1 November 2017)

Defect-free graphene nanosheets are the strongest material known but manufactured graphene tends to contain flaws of different forms and dimensions, leading to the degradation of mechanical performance. Here we report a quantitative mechanical approach to quantitatively evaluate the influence of defects within exfoliated pristine graphene sheets. Results indicate stress concentrations around defects within graphene sheets that lower strength. The description of stress concentration broadly follows a Griffith strength approach for continuum materials, despite the non-continuum structure of graphene, but has little impact on the Young's modulus.
https://doi.org/10.1063/1.4996387

Graphene has distinctive physical and chemical properties, leading to a wide range of potential applications.[1–3] The intrinsic mechanical properties of graphene are exceptional, with a measured Young's modulus of 1.0 TPa and failure strength of 130 GPa.[4] These mechanical properties highlight graphene as the strongest material known and indicate a Young's modulus and failure strength that approaches the theoretic value expected when mechanical performance is defined by material inherent chemical bonding. However, the failure of most materials is determined by the presence of defects, of different forms and length scales, instead of chemical bonds. Establishing relationships between the fracture of graphene and the role of defects is important in both understanding the mechanical performance of graphene in applications and more fundamental studies examining the suitability of continuum behavior, typically used in mechanical evaluations, to a non-continuum 2D material.

Monolayer graphene sheets presents challenges in experimental studies of mechanical performance due to low stability and rigidity. Previous works have provided methodologies to quantitatively measure the intrinsic properties of graphene using atomic force microscopy (AFM) nanoindentation,[4–6] although recent investigation indicated limitations in such approach.[7] The nanoindentation method has been exploited to examine the mechanical properties for a range of graphene materials including chemical vapor deposition graphene,[8] reduced graphene oxide,[9] which all contain a range of defects. For example, CVD graphene contains severely disordered grain boundaries with pentagonal and heptagonal structures.[8,10,11] Functional groups and distorted sp^2 structure can be observed in GO and reduced graphene.[12] As a result, the mechanical properties of defective graphene materials are expected to degrade due to the presence of defects.[8,9,11,13] These experimental studies have provided evidence that defects can significantly influence their mechanical performance, but correlations between structure and mechanical performance are limited due to the variability of graphene defects,[8–11] as well as the need to quantitatively determine their sizes and distributions.[10–14]

In this paper, we report a quantitative approach to evaluate the influence of defects on graphene. The approach uses graphene as a 'model' sheet and controllably introduces defects using focused ion

[a]asa.barber@port.ac.uk

beam (FIB) based method. FIB is advantageous as the introduced defect is defined so that accurate determination of the effect of a defect on graphene mechanics can be made. The mechanical properties of graphene with such defects were further measured using AFM nanoindentation to obtain mechanical relationships.

Pristine graphene were routinely deposited, examined and confirmed by Raman spectroscopy.[15,16] Fig. 1(a) and (b) shows the optical image of the deposited graphene and the corresponding Raman spectrum. A single nanoscale defect was introduced into a monolayer graphene using FIB milling with a pre-defined dimension and position. Defects were positioned at quarter hole diameters and set at 100 ± 15 nm in diameter as direct observations and schematic in Fig. 1 (c) and (d). The mechanical properties including failure strength and Young's modulus were measured based on AFM nanoindentation. A total of 5 isolated graphene sheets with introduced defect and 5 pristine graphene sheets were tested.

Fig. 2 (a) and (b) shows the SEM image of defective graphene covered the pre-patterned holes on silicon substrate to form the suspended graphene and corresponding AFM topographic image prior to mechanical testing. Fig. 2 (c) shows the height profile of the dash line that crossed the introduced defect in Fig. 2 (b). The graphene is noted as adhered to the vertical wall of the hole by 8 ~ 12 nm, which can be attributed to van der Waals attraction. The defect within graphene sheet can be further identified as a significant reduction in the height profile. After acquiring topographic AFM image of suspended defective graphene, the AFM tip was moved to the geometric center of the sheet and displaced to provide nanoindentation test. Representative nanoindentation force-displacement curves for both defective and pristine graphene are shown in Fig. 3.

A clamped circular sheet, made of a linear isotropic elastic material, under central point loading is considered as the physical model for nanoindentation following the mathematical model developed

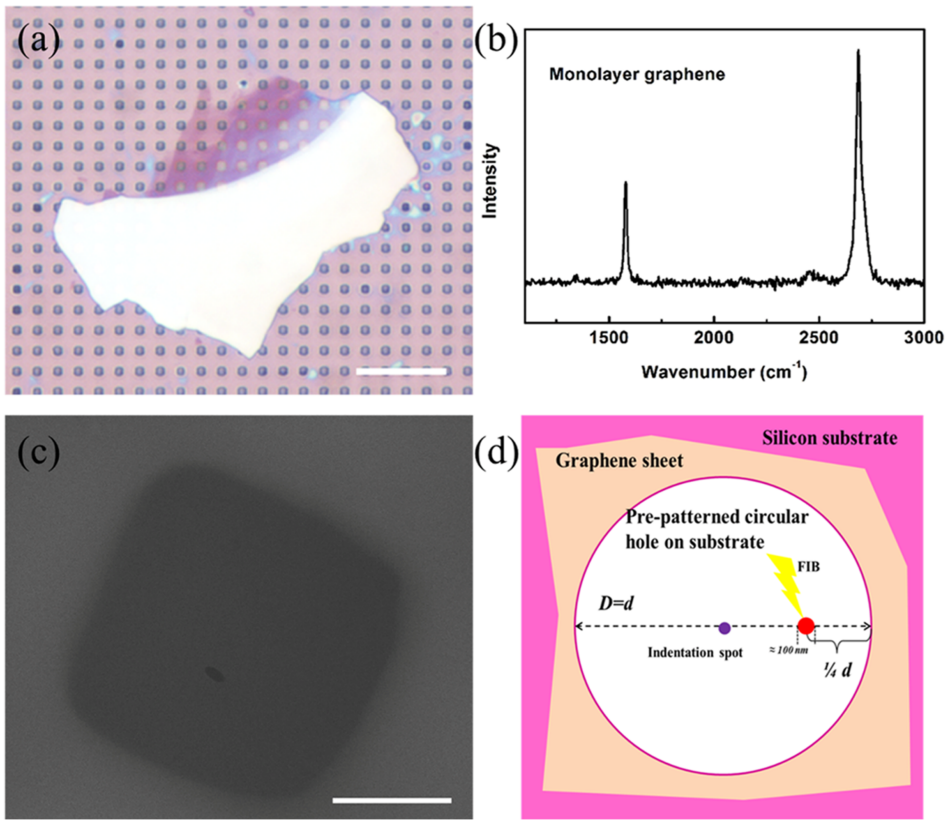

FIG. 1. (a) Optical image of deposited graphene, scale bar: 12 μm, (b) Raman spectrum of monolayer graphene, (c) SEM image of defective graphene, scale bar: 500 nm, (d) Schematic of the FIB-introduced defect on suspended graphene.

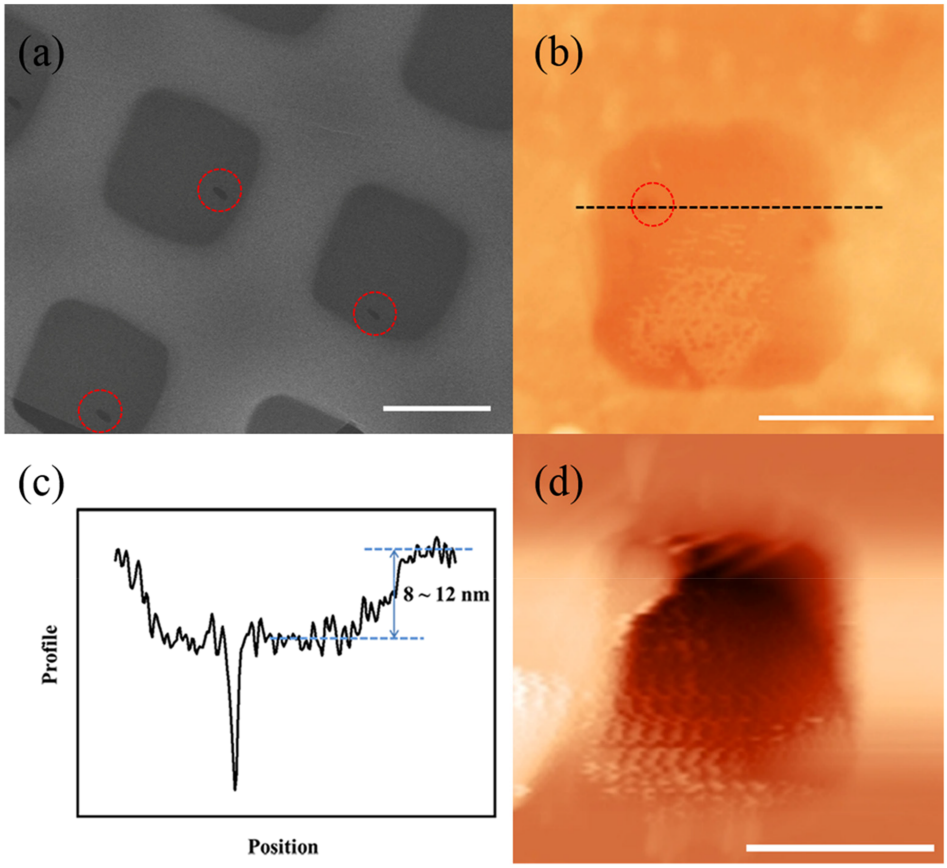

FIG. 2. (a) SEM image with defect highlighted in red circle, scale bar: 1μm, (b) AFM topographic image, (c) Height profile of the black dash line in (b), (d) AFM image of a fractured graphene after nanoindentation, scale bar: 1 μm.

by C. Lee et al.[4] The resultant mechanical force-displacement behaviour during indentation can be approximated as:[4,17,18]

$$F = \sigma_o^{2D}(\pi a)(\frac{\delta}{a}) + E^{2D}(q^3 a)(\frac{\delta}{a})^3 \quad (1)$$

where F is applied force, δ is the deflection at the centre point, ${\sigma_0}^{2D}$ is the pre-tension, ν is the sample's Poisson's ratio (taken as 0.165 for graphite in the basal plane),[19] and q=1/(1.05-0.15ν-0.16^2) =1.02. The above equation is least-square fitted to the experimental indentation curves, taking ${\sigma_0}^{2D}$ and E^{2D} as free parameters, as shown in Fig. 3. The consistency of the curve fitting verifies the appropriate use of this quasi-empirical polynomial form to describe deformation and failure of a suspended graphene during indentation. It is noted that pre-patterned substrate holes are not perfectly circular shape, however, the mechanical response of graphene sheet on such quasi-circular still follow the above equation,[8] as evidenced by the consistency of curve fitting. The fitted pre-tension ${\sigma_0}^{2D}$ and Young's modulus E^{2D} for each 5 defective and pristine graphene are summarized in Table S1 in the supplementary material.

The obtained pre-tension ranges from 0.046 to 0.383 N.m^{-1}, which is comparable and in good agreement with previous measurements.[4,8,11] The force required to fail the defective graphene is around 70-180 nN, which is significantly lower than that of pristine graphene, 1600-2000 nN. Images of defective graphene before and after failure are shown in Fig. 2 (b) and (d), which highlighted a lack of slippage between the graphene at the periphery of the substrate hole. Moreover, the consistency of the experimental curves fitting even at high deflections indicates sufficient interaction between graphene and substrate to prevent relative slippage.[20] The average 2D Young's modulus of defective graphene is 279 N.m^{-1}, with a standard deviation of 65 N.m^{-1}, where was the value of pristine

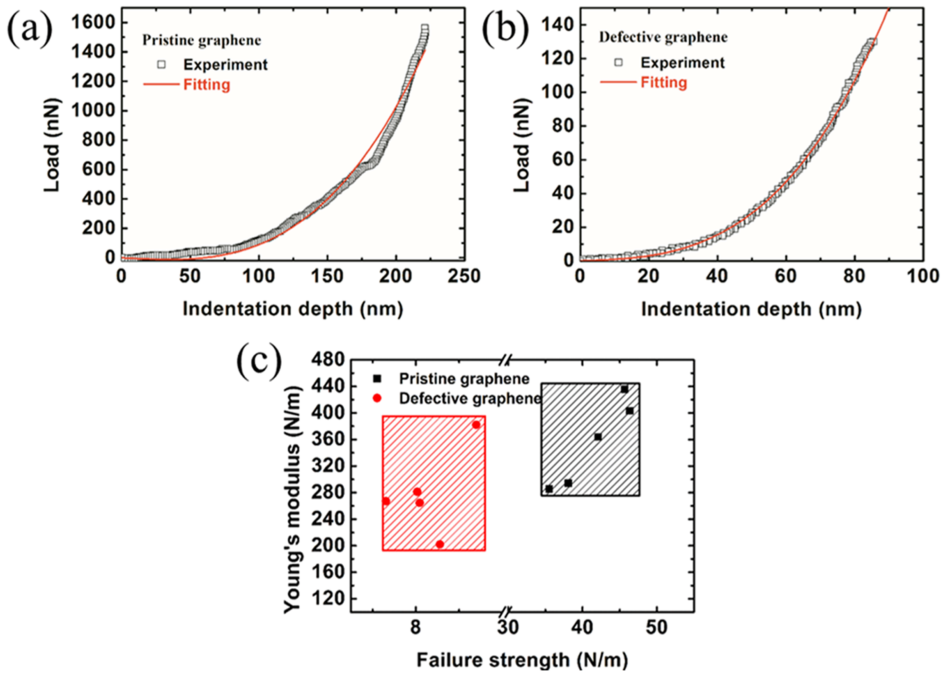

FIG. 3. Representative force-displacement curves of (a) pristine (b) defective graphene. (c) Summary of measured Young's modulus and failure strengths of both defective and pristine graphene.

graphene is 356 ± 66 N.m^{-1}. This measured 2D Young's modulus of defective graphene corresponds to 0.84 ± 0.18 TPa in 3D assuming a graphene thickness of 0.335 nm. Considering the large overlapping range of measured Young's modulus, as shown in Fig. 3(c), we can conclude that the introduced defect has fewer influence on Young's modulus of graphene sheets.

The failure strength of graphene was evaluated by considering a clamped, linear elastic, circular membrane under a spherical indenter as a function of applied load and the geometry of indenter:[4]

$$\sigma_f^{2D} = \left(\frac{FE^{2D}}{4\pi R}\right)^{\frac{1}{2}} \tag{2}$$

Specifically, failure strength is proportional to the failure load while varies inversely with tip radius. In our work, the radius of the AFM tip is 35 ± 3 nm, as shown in Fig. S1 in the supplementary material. The calculated average strength is 42 and 8.55 N.m^{-1} for pristine and defective graphene respectively, both of which are overestimated since Equation (2) ignores nonlinear elasticity.[4,11] However, the failure strength of defective graphene is still approximately one fifth of that for pristine graphene from Equation (2) calculation, indicating the introduced defects could significantly reduce the graphene strength.

In conventional 3D materials, the effect of defect on strength can be evaluated based on Griffith theory. Introducing Griffith theory to graphene is non-ideal as graphene may not conform to a continuum material. However, the occurrence of brittle failure when the decrease of strain energy exceeds the increase of surface energy of an infinitesimal crack, resulting in crack propagation for failure, is expected to be conceptually valid for graphene. Consideration of graphene as an elastic body containing an internal crack of length $2a_0$ subjected to external load, allows the failure strength to be written as:

$$\sigma_f = \sqrt{\frac{2\gamma E}{\pi a_0}} \tag{3}$$

where γ is the 2D edge free energy, E is the Young's modulus and a_0 is the crack half length. Equation (3) assumes the graphene deform uniaxially under AFM nanoindentation, while the stress is expected to be complex around the indenting tip, a sheet straining uniaxially can be approximately

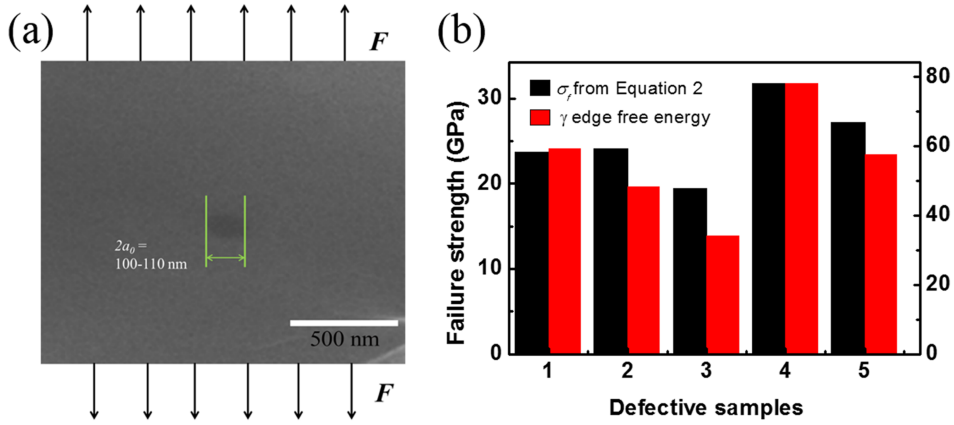

FIG. 4. (a) SEM image of a defect within graphene under an assumed uniaxial loading condition, (b) Comparison of failure strength derived from Equation (2) and calculated 2D edge free energy γ.

correct when considering the deformed sheet as a 1D 'string' unit under a point load as shown in Fig. S2 in the supplementary material. SEM image shows the dimension of the introduced defect in Fig. 4(a), assuming the graphene is under uniaxial tensile stress. The Griffith Equation (3) can be rewritten as,

$$\sigma_f \sqrt{a_0} = \sqrt{\frac{2\gamma E}{\pi}} \tag{4}$$

where the left side of Equation (4) only contains the experimental quantities while the right side depends on the intrinsic properties of the material. As listed in Table I, the measured values of $\sigma_f \sqrt{a_0}$ ranges from 4.7 to 7.2 MPa$\sqrt{\text{m}}$ and are distributed evenly around an average value of 5.8 MPa$\sqrt{\text{m}}$ with a standard deviation (s. d.) of 0.9 MPa$\sqrt{\text{m}}$. Considering the difficulties and uncertainties associated with sample preparation and methodology simplification, these results indicate that the measured $\sigma_f \sqrt{a_0}$ could be considered as a constant. Therefore, our findings provide a direct evidence that classic Griffith theory could also applicable in low dimensional non-continuum graphene materials. Taking the above measured $\sigma_f \sqrt{a_0}$ and E to Equation (3), γ, the 2D edge free energy of graphene could be extracted accordingly, which ranges from 34 to 78 J m^{-2} and an average value of 55.5 J m^{-2} with a standard deviation (s. d.) of 16.1 J m^{-2}, as shown in Table I and Figure 4(b).

Since brittle fracture behavior was observed here for graphene, the practical strength is governed by the fracture toughness characterized by the critical energy release rate, G_c.[21] The critical energy release rate assumes that the critical energy supplied to the crack tip during growth must be balanced by the amount of energy dissipated due to the formation of new surfaces. In our case, G_c can be written as:[22]

$$G_c = \sigma_f^2 \pi a_0 / E \tag{5}$$

TABLE I. Experimental data obtained from nanoindentation on defective graphene sheets and results from application of Griffith theory.

Defective graphene No.	Half crack length a_o (nm)	Failure strength σ_f (GPa)	$\sigma_f \sqrt{a_0}$ (MPa$\sqrt{\text{m}}$)	Edge free energy γ (J m^{-2})	Energy release rate G_c (J m^{-2})
1	56	24.1	5.7	49.9	99.7
2	53	24.4	5.6	48.4	96.8
3	57	19.7	4.7	34.0	68.1
4	49	32.2	7.2	78.1	156.1
5	50	27.5	6.1	57.6	115.2

Therefore, the critical energy release rate is proportional to the square of failure strength and the crack length. For each defective graphene sheets, G_c could be calculated according to Equation (5), as exhibited in Table I. The average energy release rate for defective graphene is about 107 J m^{-2} with a standard deviation of 32.3 J m^{-2}, as shown in Table I. This failure strength obtained from Equation (2) is noted as potentially providing an overestimation due to ignoring plasticity.

In summary, defective graphene sheets were prepared using FIB applied to exfoliated pristine graphene. The fabricated defective graphene were mechanically tested by AFM nanoindentation and the resultant force-displacement curves used to extract the mechanical properties, particularly the failure strength as well as Young's modulus. The Young's modulus of defective graphene was comparable to pristine graphene whereas the failure strength was significantly lower than pristine graphene. However, similarities between the experimentally derived failure strength and Griffith theory incorporating the size of the defected into a calculated failure strength was found. This result indicates that defects within graphene sheets result in stress concentrations that lower strength, as for continuum materials. The influence of the size of the defect on the strength reduction for single graphene sheets appears to be broadly described by Griffith theory.

See supplementary material for the more details about the preparation of pristine and defective graphene and nanoindentation testing.

This work was partially supported by National Natural Science Foundation of China (51502320), Natural Science Foundation of Shanxi Province (201601D021060) and Shanxi Scholarship Council of China.

[1] S. P. Pang, Y. Hernandez, X. L. Feng, and K. Mullen, Adv. Mater. **23**, 2779 (2011).
[2] M. D. Stoller, S. J. Park, Y. W. Zhu, J. H. An, and R. S. Ruoff, Nano Lett. **8**, 3498 (2008).
[3] T. Kuilla, S. Bhadra, D. Yao, N. H. Kim, S. Bose, and J. H. Lee, Prog. Polym. Sci. **35**, 1350 (2010).
[4] C. Lee, X. Wei, J. W. Kysar, and J. Hone, Science **321**, 385 (2008).
[5] I. W. Frank, D. M. Tanenbaum, A. M. Van der Zande, and P. L. McEuen, J. Vac. Sci. Technol. B **25**, 2558 (2007).
[6] M. Poot and H. S. van der Zant, Appl. Phy. Lett. **92**, 063111 (2008).
[7] J. Han, N. M. Pugno, and S. Ryu, Nanoscale **7**, 15672 (2015).
[8] C. S. Ruiz-Vargas, H. L. Zhuang, P. Y. Huang, A. M. van der Zande, S. Garg, P. L. McEuen, and J. Park, Nano Lett. **11**, 2259 (2011).
[9] J. W. Suk, R. D. Piner, J. An, and R. S. Ruoff, ACS Nano **4**, 6557 (2010).
[10] P. Y. Huang, C. S. Ruiz-Vargas, A. M. van der Zande, W. S. Whitney, M. P. Levendorf, J. W. Kevek, and D. A. Muller, Nature **469**, 389 (2011).
[11] G. H. Lee, R. C. Cooper, S. J. An, S. Lee, A. van der Zande, N. Petrone, and J. Hone, Science **340**, 1073 (2013).
[12] D. R. Dreyer, S. Park, C. W. Bielawski, and R. S. Ruoff, Chem. Soc. Rev. **39**, 228 (2010).
[13] C. Wang, M. D. Frogley, G. Cinque, L. Q. Liu, and A. H. Barber, Nanoscale **6**, 14404 (2014).
[14] A. Zandiatashbar, G. H. Lee, S. J. An, S. Lee, N. Mathew, M. Terrones, and N. Koratkar, Nat. Commun. **5** (2014).
[15] K. S. Novoselov, D. Jiang, F. Schedin, T. J. Booth, V. V. Khotkevich, S. V. Morozov, and A. K. Geim, P. Natl. Acad. Sci. USA **102**, 10451 (2005).
[16] A. C. Ferrari, J. C. Meyer, V. Scardaci, C. Casiraghi, M. Lazzeri, F. Mauri, and A. K. Geim, Phys. Rev. Lett. **97**, 187401 (2006).
[17] M. R. Begley and T. J. Mackin, J. Mech. Phys. Solids **52**, 2005 (2004).
[18] U. Komaragiri, M. R. Begley, and J. G. Simmonds, J. Appl. Mech. **72**, 203 (2005).
[19] O. L. Blakslee, D. G. Proctor, E. J. Seldin, G. B. Spence, and T. Weng, J. Appl. Phys. **41**, 3373 (1970).
[20] C. Lee, X. Wei, Q. Li, R. Carpick, J. W. Kysar, and J. Hone, Phys. Status Solidi B **246**, 2562 (2009).
[21] P. Zhang, L. Ma, F. Fan, Z. Zeng, C. Peng, P. E. Loya, and J. Lou, Nat. Commun. **5** (2014).
[22] T. Anderson, *Fracture Mechanics: Fundamentals and Applications*, 3rd edn (CRC Press, 2004).